

Electrocatalytic properties of palladium modified zinc oxide nanorods (Pd-ZnO NRs): Hydrothermal preparation and characterization

K. Suresh Babu^a, T. Dhanasekaran^a, A. Padmanaban^a, G. Gnanamoorthy^a, A. Stephen^b and V. Narayanan^{a*}

^aDepartment of Inorganic Chemistry, ^bDepartment of Nuclear Physics,
University of Madras, Guindy Campus, Chennai-600 025, India

E-mail: vnnara@yahoo.co.in

Manuscript received online 28 August 2018, accepted 09 October 2018

Among various semiconductor materials, zinc oxide (ZnO) presents itself as one of the most important semiconductor due to its versatile potential properties, when modified with palladium has attracted much attention for their promising applications. Nano rods (NRs) like structure were prepared through hydrothermal method. As synthesized samples morphological properties were characterized by X-ray diffraction (XRD), diffuse reflectance ultra-violet spectroscopy (DRS-UV), photo luminescence (PL), field emission scanning electron microscope (FE-SEM), high resolution transmission electron microscope (HR-TEM) in order to confirm the phase purity and surface morphology of the sample. Palladium modified ZnO NRs (Pd-ZnO) samples possess a stable morphological structure composed of rod like structure. The modified glassy carbon (GC) electrode with Pd-ZnO NRs shows better catalytic activity for the electrochemical oxidation of uric acid (UA).

Keywords: Zinc oxide nanorods, palladium, electrocatalytic properties, glassy carbon.

Introduction

In semiconductor metal oxide (SMO) the age-old goal to study the interaction between the metal nanoparticles (NPs)-SMO interactions remains a face up to task. Size and defect control, besides the distribution of the metal NPs on SMO is always a challenge and the outcomes of this, influences the most promising properties like optical, electronic and catalytic to prepare outstanding metal NPs-SMO^{4,6,9,10}. Indeed, noble metal NPs decoration on SMO promotes the activity of SMO^{1,2,5,8}. The recombination of electron-hole pair is being delayed by electron sink noble metal nanoparticles in noble metal NP-SMO. Among various SMO, the wurtzite hexagonal structured ZnO presents itself as one of the most important II-VI group, due to its a variety of properties such as wide band gap of 3.37 eV, large exciton binding energy of 60 meV, much higher than other SMO^{14,15}.

In this present study we have reported the preparation of Pd modified ZnO nanorods, using a hydrothermal method. The prepared nanoparticles is used to modify the GC electrode. The modified GC electrode shows better catalytic activity for the electrochemical oxidation of UA when compared with the bare GC electrode.

Experimental

Synthesis of Pd modified ZnO (Pd-ZnO):

Precursors, $\text{Zn}(\text{CH}_3\text{COO})_2 \cdot 2\text{H}_2\text{O}$ and NaOH were dissolved into of distilled water to which PdCl_2 were added. After the mixture was magnetically stirred, was transferred into a Teflon lined stainless steel autoclave. It was then sealed and maintained at 180°C for 2 h. After separation the samples were finally calcined at 200°C for 2 h. All the reagents were analytical grades. Deionized water was used in the experiments.

Characterization:

To analyse the sample structure a Rich Siefert 3000 diffractometer with $\text{Cu-K}_{\alpha-1}$ radiation ($\lambda=1.5406 \text{ \AA}$) was used. The surface morphology of the prepared sample was analyzed by FE-SEM using a HITACHI SU6600 field emission-scanning electron microscopy and TEM using a PHILIPS CM200 transmission electron microscopy respectively. The electrocatalytic experiments were performed on a CHI 600A electrochemical instrument using as-coated electrodes and bare GCE, a platinum wire was the counter electrode and saturated calomel electrode (SCE).

Results and discussion

Characterization: Fig. 1 depicts XRD patterns of the as-prepared, palladium modified ZnO samples. The peaks diffraction at 31.8°, 34.4°, 36.3°, 47.5°, 56.6°, 62.9°, 66.4°, 68.0°, 69.1° can be indexed to the planes of standard patterns for hexagonal phase wurtzite structure ZnO (JCPDS Card File No. 36-1451) and at 40.1° can be indexed to face-centered cubic (fcc) of palladium (JCPDS 05-0681), according to the reported data. All the peaks agree well with two crystal phases and no other characteristic peaks are observed, indicating high purity of the as-prepared samples. The come out sug-

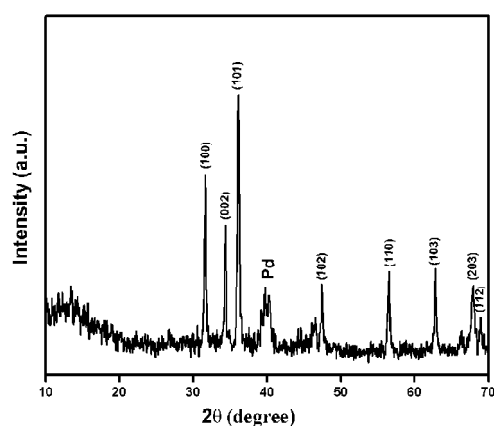


Fig. 1. XRD patterns Pd-ZnO NRs.

gests that the obtained products are palladium modified ZnO NRs. The room temperature photoluminescence spectrum for colloidal solution of the sample at 340 nm of excitation energy is shown in Fig. 2. Luminescence peaks centred at

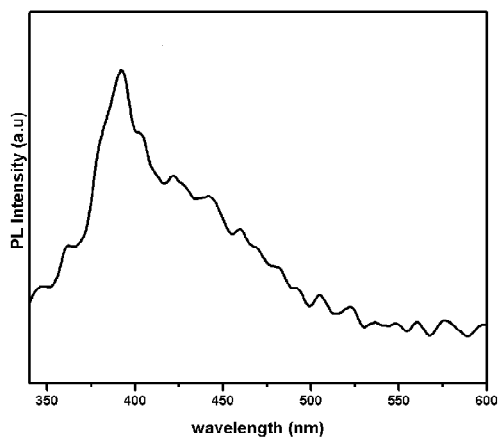


Fig. 2. PL spectrum of Pd-ZnO NRs.

392 nm has been observed for the prepared samples, due to the radiative recombination of an electron and a hole, i.e. the excitonic emission^{7,13}. As-prepared Pd modified ZnO sample shows a prominent excitonic absorption peak at 355 nm at room temperature against the optical absorption spectra is shown in the Fig. 3. This may be attributed due to the quantum size effects in nanocrystals^{3,11}. The variation of $(\alpha hv)^2$

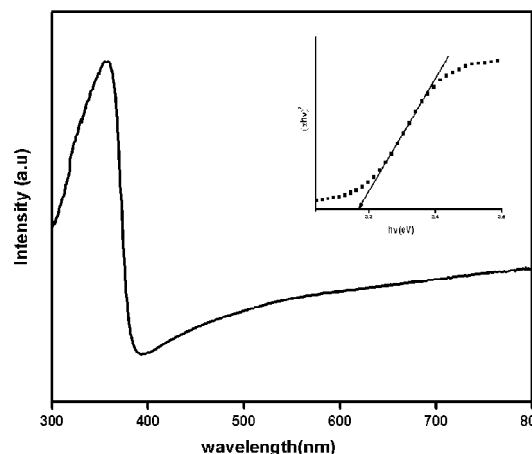


Fig. 3. DRS UV-Visible spectrum; inset plots of $(\alpha hv)^2$ vs photon energy (hv).

versus photon energy (hv) for the synthesized sample is plotted in Fig. 3 (inset). The band gap (E_g) is estimated through the extrapolation method¹⁴. The values is found to be 3.28 eV. Fig. 4 depicts FESEM of the sample are in rod like structure. HRTEM reinforces the rod like structure and the distribution of palladium particles in the ZnO rods shown in Fig. 5. Fig. 6 depicts EDX spectrum of the sample confirms presence of Pd, Zn and O elements.

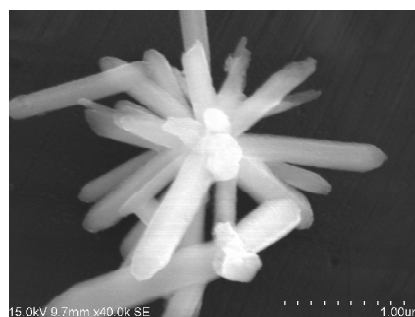


Fig. 4. FE-SEM image of Pd-ZnO NRs.

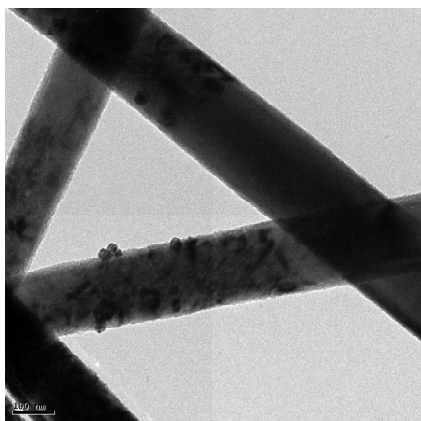


Fig. 5. HR-TEM image of Pd-ZnO NRs.

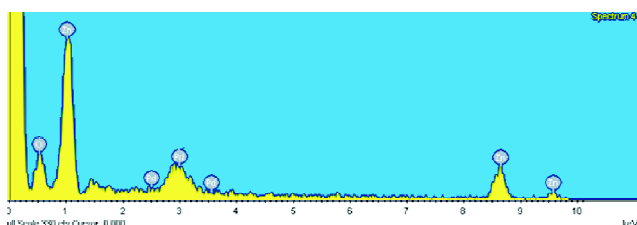


Fig. 6. EDAX spectrum of Pd-ZnO NRs.

Electrochemical oxidation of uric acid at the Pd-ZnO NRs coated electrode:

The modified electrodes show shift in anodic peak potential with enhanced anodic peak current than the bare GCE, indicates that the modified electrode (Pd-ZnO NRs/GCE) has better catalytic activity shown in Fig. 7. The oxidation peak potential and anodic peak current of UA at Pd-ZnO NRs/GCE

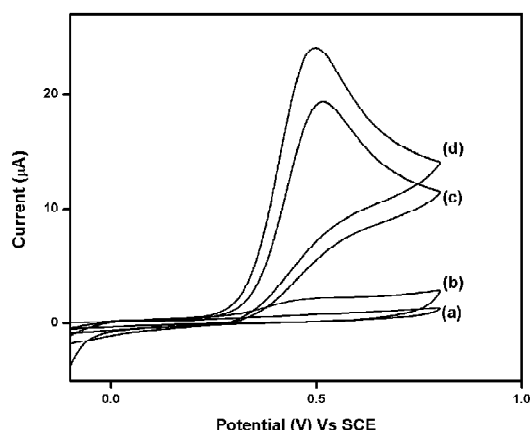


Fig. 7. CVs of (a) bare GCE and (b) Pd-ZnO NRs/GCE in 0.1 MPBS (pH 7.0), (d) Pd-ZnO NRs in 0.1 MPBS (pH 7.0) solution containing 1.0 mM uric acid at scan rate 50 mV s⁻¹.

is about 0.49 V and 24 mA respectively, which is higher than bare GCE and comparable with the reported catalyst^{12,16}. Consequently, the results suggest that Pd-ZnO NRs enhance the electron transfer rate and lower the overpotential of UA oxidation. Effect of scan rate were also studied. From Fig. 8, it can be seen that the oxidation peak current moved linearly with increasing scan rate in the range from 30 to 700 mV s shows an adsorption-controlled.

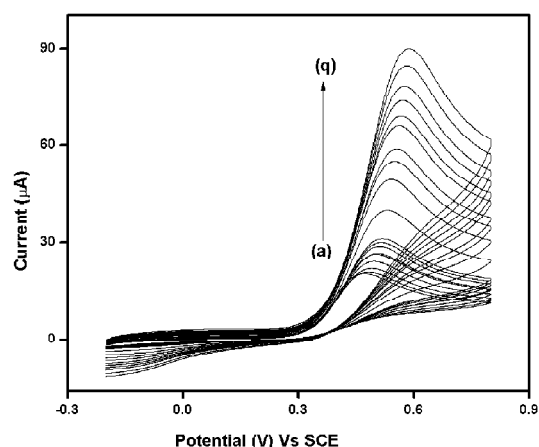


Fig. 8. CV of Pd-ZnO NRs/GCE at the scan rate (a) 20, (b) 30, (c) 40, (d) 50, (e) 60, (f) 70, (g) 80, (h) 90, (i) 100, (j) 150, (k) 200, (l) 250, (m) 300, (n) 350 (o) 400 (p) 450 (q) 500 mV s⁻¹.

Conclusions

Pd modified ZnO NRs were prepared by hydrothermal method. The characterization techniques confirms the modification of ZnO by palladium. Pd-ZnO NRs covered GC electrodes were successfully fabricated. The as-prepared Pd-ZnO NRs/GCE show an excellent electro-catalytic activity towards the oxidation of UA. As-prepared sample, favors for the anodic peak potential and current increment.

References

1. Uri Banin, Yuval Ben-Shahar and Kathy Vinokurov, *Chemistry of Materials*, 2013, **26**, 97.
2. Chia-Ming Chang, Min-Hsiung Hon and Ing-Chi Leu, *ACS Applied Materials & Interfaces*, 2012, **5**, 135.
3. Yonggang Chang, Jian Xu, Yunyan Zhang, Shiyu Ma, Lihui Xin, Lina Zhu and Chengtian Xu, *J. Phys. Chem. C*, 2009, **113**, 18761.
4. S. Choopun, R. D. Vispute, W. Noch, A. Balsamo, R. P. Sharma, T. Venkatesan, A. Iliadis and David C. Look, *Appl. Phys. Lett.*, 1999, **75**, 3947.

Suresh Babu *et al.*: Electrocatalytic properties of palladium modified zinc oxide nanorods (Pd-ZnO NRs):

5. Joseph F. S. Fernando, Matthew P. Shortell, Kristy C. Vernon, Esa A. Jaatinen and Eric R. Waclawik, *Crystal Growth and Design*, 2015, **15**, 4324.
6. Myrtil L. Kahn, Miguel Monge, Vincent Collière, Francois Senocq, André Maisonnat and Bruno Chaudret, *Advanced Functional Materials*, 2005, **15**, 458.
7. Jasmeet Kaur, Praveen Kumar, Thangaiah Stephen Sathiaraj and Rengasamy Thangaraj, *International Nano Letters*, 2013, **3**, 4.
8. Martti Kauranen and Anatoly V. Zayats, *Nature Photonics*, 2012, **6**, 737.
9. Charles M. Lieber, *Solid State Communications*, 1998, **107**, 607.
10. Yoshitake Masuda and Kazumi Kato, *Crystal Growth and Design*, 2008, **8**, 2633.
11. R. Suresh, K. Giribabu, R. Manigandan, S. Munusamy, S. Praveen Kumar, S. Muthamizh, A. Stephen and V. Narayanan, *Journal of Alloys and Compounds*, 2014, **598**, 151.
12. R. Suresh, K. Giribabu, R. Manigandan, A. Stephen and V. Narayanan, *RSC Advances*, 2014, **4**, 17146.
13. J. J. Wu, H. I. Wen, C. H. Tseng and S. C. Liu, *Advanced Functional Materials*, 2004, **14**, 806.
14. Sheng Xu and Zhong Lin Wang, *Nano Research*, 2011, **4**, 1013.
15. Noboru Yamazoe, *Sensors and Actuators B: Chemical*, 1991, **5**, 7.
16. Guangming Yang, Lin Tan, Ya Shi, Suiping Wang, Xuxiao Lu, Huiping Bai and Yunhui Yang, *Bull. Korean Chem. Soc.*, 2009, **30**, 454.